

Research article

Open Access

Zone center phonons of the orthorhombic RMnO_3 ($R = \text{Pr, Eu, Tb, Dy, Ho}$) perovskites

HC Gupta*¹ and Upendra Tripathi²Address: ¹Physics Department, Indian Institute of Technology, Hauz Khas, New Delhi, India and ²Physics Department, Amity University, Noida, UttarPradesh, IndiaEmail: HC Gupta* - hcgupta@physics.iitd.ernet.in; Upendra Tripathi - t_upendra1974@yahoo.co.in

* Corresponding author

Published: 17 March 2008

Received: 2 November 2007

PMC Physics B 2008, 1:9 doi:10.1186/1754-0429-1-9

Accepted: 17 March 2008

This article is available from: <http://www.physmathcentral.com/1754-0429/1/9>

© 2008 Gupta and Tripathi

This is an Open Access article distributed under the terms of the Creative Commons Attribution License (<http://creativecommons.org/licenses/by/2.0>), which permits unrestricted use, distribution, and reproduction in any medium, provided the original work is properly cited.

Abstract

A short range force constant model (SRFCM) has been applied for the first time to investigate the phonons in RMnO_3 ($R = \text{Pr, Eu, Tb, Dy, Ho}$) perovskites in their orthorhombic phase. The calculations with 17 stretching and bending force constants provide good agreement for the observed Raman frequencies. The infrared frequencies have been assigned for the first time.

PACS Codes: 36.20.Ng, 33.20.Fb, 34.20.Cf

Introduction

Until recently the RMnO_3 perovskites ($R = \text{rare earth elements}$) have been the object of research mainly as parent materials of mixed valence manganites exhibiting colossal magnetoresistivity (CMR) [1-4]. In the past few years, however, there is an increased interest in the complex relationships among the lattice distortions, magnetism, dielectric, and transport properties of undoped RMnO_3 [5-10]. All RMnO_3 perovskites show a distortion of MnO_6 octahedra due to orbital ordering characteristic of the Jahn-Teller effect of Mn^{3+} cations [11-15]. An investigation of infrared and Raman frequencies will be quite useful in describing the details of such properties. Practically, very limited information is available on the infrared and Raman scattering of orthorhombic RMnO_3 . Martin Carron *et al.* [11] studied the behavior of Raman phonons through the transition from static to dynamic Jahn-Teller order in stoichiometric RMnO_3 samples ($R = \text{La, Pr, Y}$). Also Martin Carron *et al.* [12] studied orthorhombic RMnO_3 ($R = \text{Pr, Nd, Eu, Tb, Dy, Ho}$) manganites for their Raman phonons as a function of the rare earth ions and temperature. They had assigned only some of the Raman modes. They correlated the frequencies of three most intense modes of orthorhombic samples, with some structural parameters such as Mn-O

bond distances, octahedral tilt angle and Jahn-Teller distortion. Further rationalization of the Raman spectra of orthorhombic RMnO_3 ($R = \text{Pr, Nd, Tb, Ho, Er}$) and different phases of Ca- or Sr-doped RMnO_3 compounds as well as cation deficient RMnO_3 were made by Martin Carron *et al.* [13]. Their assignment of the peaks related to octahedral tilt were in good agreement with the other authors but the assignment of peak to an antisymmetric stretching associated with the Jahn-Teller distortion was doubtful. Wang Wei-Ran *et al.* [14] measured Raman active phonons in orthorhombic RMnO_3 ($R = \text{La, Pr, Nd, Sm}$) compounds and they also assigned three main Raman peaks. Recently, the polarized Raman spectra of orthorhombic RMnO_3 ($R = \text{Pr, Nd, Eu, Gd, Tb, Dy, Ho}$) series at room temperature were studied by Iliev *et al.* [15] where they had assigned the observed frequencies to nine Raman modes. Their study shows that the variations of lattice distortions with radius of rare earth atoms affect significantly both the phonon frequencies and the shape of some of Raman modes. To our knowledge, the theoretical investigations of phonons, using the normal coordinate analysis in the orthorhombic NdMnO_3 has first been made by Gupta *et al.* [16].

In the present study, the theoretical investigations of phonons in the orthorhombic RMnO_3 have been made using the normal coordinate analysis. It has been observed that a total of 17 inter-atomic force constants, which include 8 bending force constants, are enough to obtain a good agreement between theory and experiment for the Raman frequencies. The assignments of infrared frequencies along with their corresponding eigen vectors observing the atomic displacements in the respective vectors have been made for the first time. There is always some scope of more precise infrared experiments to verify these theoretical values.

Theory

The structure of stoichiometric RMnO_3 shown in Fig. 1, described at room temperature by the $Pbnm$ space group ($Z = 4$), can be considered as orthorhombically distorted superstructure of ideal perovskites. In the $Pbnm$ structure the atoms occupy four non equivalent atomic sites of them only the Mn site is a center of symmetry [17]. The distortion of the orthorhombic perovskites characterized by the tilting angle of the MnO_6 octahedra progressively increases from Pr to Er due to simple steric factors. Additionally, all of the perovskites show a distortion of the MnO_6 octahedra due to orbital ordering characteristic of the Jahn-Teller of the Mn^{3+} cations. Structural data of EuMnO_3 is very recent because of its high neutron absorption and they are perfectly correlated with the other members of RMnO_3 series [18].

The total number of irreducible representations for RMnO_3 are

$$= 7A_g + 7B_{1g} + 5B_{2g} + 5B_{3g} + 8A_u + 8B_{1u} + 10B_{2u} + 10B_{3u}$$

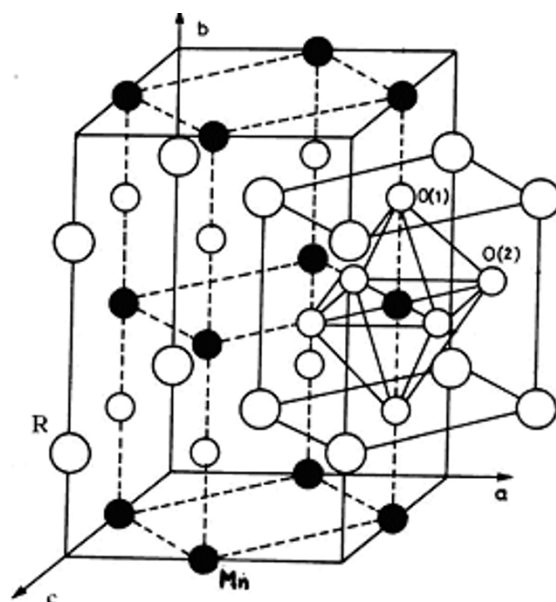


Figure 1

The structure of Orthorhombic RMnO_3 ($R = \text{Pr, Nd, Eu, Gd, Tb, Dy, Ho}$) compounds at room temperature, belonging to Pbnm space group. The structure has four formulae unit with R atoms, Mn atoms and O atoms (O1 and O2).

There are four Raman active species, $A_{g'}$, $B_{1g'}$, B_{2g} and $B_{2g'}$ three infrared active species B_{1u} , B_{2u} and B_{3u} and inactive specie A_u .

In the present paper, an attempt has been made to study the zone center phonons in RMnO_3 ($R = \text{Pr, Eu, Tb, Dy, Ho}$) for the first time using SRFCM. We have used nine valence force constants $K_1(\text{Mn-O2})$, $K_2(\text{Mn-O1})$, $K_3(\text{Mn-O2})$, $K_4(\text{R-O1})$, $K_5(\text{R-O2})$, $K_6(\text{R-O1})$, $K_7(\text{R-O2})$, $K_8(\text{R-O1})$, $K_9(\text{R-O2})$; and eight bending force constants $H_1(\text{O1-R-O1})$, $H_2(\text{O1-R-O1})$, $H_3(\text{O1-R-O1})$, $H_4(\text{O1-R-O2})$, $H_5(\text{O1-R-O2})$, $H_6(\text{O1-R-O2})$, $H_7(\text{O2-R-O2})$ and $H_8(\text{O2-R-O2})$ at various inter-atomic distances and angles as shown in Table 1 (only for PrMnO_3).

Table 1: Force constant, Coordination number, Inter-atomic Distances (Å) and Angles (deg) and Force constant values (N/cm) for Orthorhombic PrMnO_3

Force constant	K_1	K_2	K_3	K_4	K_5	K_6	K_7	K_8	K_9	H_1	H_2	H_3	H_4	H_5	H_6	H_7	H_8
Coord. Number.	8	8	8	4	8	4	8	4	8	8	8	4	4	8	8	7	8
Distance/ Angle	1.91	1.95	2.21	2.36	2.40	2.48	2.62	3.17	3.52	89	67	110	90	56	66	160	120
Force constant values	0.597	0.535	0.950	0.456	0.019	0.311	0.382	0.335	0.598	0.432	0.413	0.404	0.373	0.338	0.329	0.136	0.022

Results and Discussions

A systematic variation in the most of the force constants is seen throughout the series. It was interesting to observe that although, the interatomic distances for K_1 and K_3 between Mn and O2 atoms remain nearly unchanged from Pr to Ho but the force constant exhibited a uniform increase. This behaviour can be related to the increase in distortion of MnO_6 octahedra. Further, as shown in Table 1 the force constant K_3 (0.950 N/cm) is quite large when compared with the similar force constant obtained in studies of $NdNiO_3$ [19] and $NdGaO_3$ [20] (0.620 N/cm). A similar kind of behaviour of large force constant between Mn and O2 atoms was observed in pyrochlore manganates [21]. This may be one of the possible reasons of associated CMR properties of manganese compounds. To account for a drastic change in resistivity and a low critical temperature in such materials, it should be noted that the double exchange model must be combined with the effect of the Jahn-Teller distortion of MnO_6 octahedra [22]. This effect promotes carrier localization and dresses charge carriers *via* cloud of phonons. It is in this respect where the large interatomic force between Mn and O2 atoms plays an important role, being a part of the distortion of the MnO_6 octahedra. The force constants between R and O1 atoms, K_4 and K_6 increase with decrease of R-O1 distance almost uniformly throughout the series. The force constant K_8 (R-O1) changes by a small amount as the R-O1 distance also shows the similar behavior. The force constants K_5 , K_7 and K_9 also show a uniform increase. Although force constant K_5 is very

Table 2: *Observed [15] and Calculated Raman Wave Numbers (cm^{-1}) for Orthorhombic $RMnO_3$ (R = Pr, Eu, Tb, Dy, Ho)

Modes	*Pr	Pr	*Eu	Eu	*Tb	Tb	*Dy	Dy	*Ho	Ho
A_g	491	491	501	501	509	509	513	513	520	520
	462	462	479	479	489	489	492	492	499	499
		386		392		402		412		408
	324	324	361	361	378	378	386	386	395	395
	232	232		270		269		272	288	288
		206		205		211		213		210
B_{1g}		64		67		79		79		77
	607	607	610	610	612	612	614	614	615	615
	496	496	518	518	528	528	534	534	537	537
		486		499		501		501		503
	445	445	465	465	474	474	478	478	481	481
	312	312	324	324	331	331	336	336		340
B_{2g}		114		122		127		129		129
		84		91		96		97		97
		627		611		621		624		617
		492		511		519		521		529
		432		463		469		476		482
		283		295		302		306		309
B_{3g}		125		131		134		134		135
		537		521		545		553		546
		400		429		432		432		454
		305		367		381		390		402
		239		266		270		274		286
		123		124		127		127		125

Table 3: Calculated Infrared Wave Numbers (cm^{-1}) for Orthorhombic RMnO_3 (R = Pr, Eu, Tb, Dy, Ho)

Modes	Pr	Eu	Tb	Dy	Ho
B_{1u}	608	611	612	614	617
	569	581	581	580	582
	485	492	509	514	516
	303	323	328	332	338
	205	213	214	214	223
	141	152	158	159	161
	133	135	142	144	143
	0	0	0	0	0
B_{2u}	614	612	617	620	620
	571	582	582	580	580
	467	494	498	500	511
	389	395	406	417	410
	290	304	309	312	318
	223	229	232	234	235
	201	206	208	208	213
	177	176	180	179	178
	132	142	148	148	149
	0	0	0	0	0
B_{3u}	535	538	551	558	562
	484	505	515	519	522
	431	458	463	465	474
	343	384	398	406	419
	315	320	318	316	315
	244	268	272	277	289
	181	181	185	184	184
	131	137	143	144	143
	106	115	118	120	122
	0	0	0	0	0

small but K_9 shows comparatively a large value. The bending force constants H_1 - H_4 show a very small change in force constant values while H_7 and H_8 exhibit uniformly increasing values.

The calculated Raman frequencies in Table 2 agreed satisfactorily with the observed values [15]. The assignment of infrared frequencies as shown in Table 3 has been done for the first time. Still a precise experimental analysis of infrared frequencies is needed to verify the results of present calculations. The potential energy distribution (PED) for most of the force constant is found to be almost similar throughout the series. The PED showed that high wave numbers are dominated by stretching force constants involving Mn and O atoms and bending force constants having R and O atoms. Therefore, the symmetric stretching of the basal oxygens of the octahedra, around 610 cm^{-1} (B_{1g} symmetry); the asymmetric stretching at about 490 cm^{-1} (A_g symmetry) associated with the Jahn-Teller distortion is expected. The A_g mode (324 cm^{-1} - 395 cm^{-1}) showing a drastic increase in frequency is purely a stretching mode dominated by K_9 (R-O2). Most of the lower wave number modes have a convincing influence by R-O bending and stretching force constants. For all the compounds of the orthorhombic RMnO_3 series, we calculated the eigen vectors

Table 4: Calculated Raman Wave Numbers (cm^{-1}) of PrMnO_3 along with their Eigen-vector Lengths representing Atomic Displacements for various Atoms

Modes	Wave-numbers	Pr	Pr	O1	O1	O2	O2	O2
A_g	491	0.04	0.26	-0.08	-0.46	0.69	-0.43	0.21
	462	0.05	0.16	-0.24	0.53	0.60	0.52	-0.02
	386	0.05	0.05	0.96	0.05	0.20	0.15	0.01
	324	0.12	-0.15	-0.06	-0.66	0.09	0.54	-0.47
	232	-0.30	0.21	-0.03	-0.27	-0.18	0.47	0.74
	206	0.91	-0.16	-0.04	-0.01	-0.07	0.06	0.36
	64	0.24	0.90	0.00	-0.01	-0.27	0.01	-0.25
B_{1g}	607	-0.03	0.10	-0.06	0.96	-0.05	0.09	0.24
	496	0.33	0.05	0.78	0.06	-0.49	-0.13	-0.10
	486	0.05	0.00	0.10	-0.08	-0.07	0.99	-0.03
	445	0.07	-0.17	0.51	0.06	0.82	0.01	0.14
	312	-0.27	0.34	0.15	-0.25	-0.12	0.00	0.84
	114	0.28	0.90	-0.05	-0.01	0.24	0.00	-0.23
	84	0.85	-0.18	-0.30	-0.07	0.01	-0.01	0.38
B_{2g}	627	0.01	0.90	0.90	0.13	0.37	0.20	0.20
	493	0.08		-0.20	0.95	0.20	-0.06	
	432	-0.17		-0.27	-0.25	0.88	-0.25	
	283	0.09		-0.28	-0.05	0.19	0.94	
	125	0.98		-0.01	-0.12	0.11	-0.13	
B_{3g}	537	0.06		0.59	0.41	0.68	-0.08	
	400	0.04		-0.23	-0.69	0.64	0.25	
	305	0.21		-0.73	0.41	0.32	-0.40	
	239	0.28		-0.18	0.39	0.00	0.86	
	123	0.93		0.19	-0.20	-0.14	-0.18	

representing the displacements of various atoms. It was observed that for larger wave numbers, the displacement of O atoms is important whereas for smaller wave numbers, the displacement of R atoms dominates as given in Table 4 and Table 5 only for PrMnO_3 . Vibrations of several atoms are involved in some middle order modes.

Table 5: Calculated Infrared Wave Numbers (cm^{-1}) of PrMnO_3 along with their Eigen-vector Lengths representing Atomic Displacements for various Atoms

Modes	Wave-numbers	Mn	Mn	Mn	Pr	Pr	O1	O1	O2	O2	O2
B_{1u}	606	-0.02	-0.02	0.01	-0.10		0.95		0.11	-0.06	0.25
	569	0.02	-0.53	0.03	0.01		-0.10		0.84	-0.04	-0.02
	485	0.08	-0.05	-0.27	-0.07		0.09		0.03	0.94	-0.16
	303	-0.19	0.01	-0.17	-0.35		-0.26		0.02	0.12	0.86
	205	0.95	0.01	0.20	-0.20		-0.05		-0.01	0.00	0.15
	141	-0.24	-0.25	0.76	-0.48		-0.01		-0.17	0.17	-0.12
	133	-0.07	0.81	0.23	-0.14		-0.04		0.50	0.08	-0.07
	0	0.00	0.00	0.47	0.76		0.00		0.00	0.26	0.36
B_{2u}	614	-0.01	-0.03	0.00	0.07	0.04	0.02	0.93	-0.25	0.14	0.00
	571	0.02	-0.53	0.02	0.06	-0.06	0.00	-0.14	-0.01	0.83	-0.04
	467	-0.01	-0.01	-0.03	-0.03	-0.30	-0.22	0.21	0.88	0.03	0.18
	389	-0.04	0.00	0.10	-0.04	-0.07	0.96	0.01	0.19	0.01	0.12
	290	-0.27	0.01	-0.08	-0.10	0.03	-0.08	-0.24	-0.15	0.02	0.91
	223	-0.14	0.42	0.00	0.81	-0.32	0.01	-0.08	-0.06	0.17	0.02
	201	0.93	0.10	0.19	0.06	-0.06	-0.01	-0.07	-0.05	0.03	0.28
	177	-0.20	0.04	0.97	-0.07	-0.03	-0.12	0.00	-0.01	0.01	0.00
	132	-0.02	0.56	-0.08	-0.56	-0.46	-0.01	0.01	-0.17	0.35	-0.10
	0	0.00	0.47	0.00	0.00	0.76	0.00	0.00	0.26	0.36	0.00
B_{3u}	535	-0.25	0.07	-0.04	-0.21	-0.07	0.27	0.59	-0.49	0.46	-0.09
	484	0.15	-0.05	0.10	-0.28	0.03	0.85	-0.21	-0.10	-0.33	0.09
	431	-0.21	0.10	-0.04	-0.04	0.19	0.30	0.16	0.81	0.35	-0.04
	343	-0.04	-0.53	-0.03	-0.20	0.22	-0.14	0.57	0.15	-0.45	0.25
	315	0.05	0.82	-0.02	-0.12	0.13	-0.09	0.25	0.01	-0.31	0.35
	244	-0.25	-0.14	-0.01	0.21	-0.19	0.07	-0.16	-0.05	0.24	0.86
	181	-0.26	0.03	0.95	0.14	0.05	-0.03	0.06	0.00	-0.07	-0.05
	131	-0.06	-0.03	-0.06	0.12	0.93	0.00	-0.19	-0.24	0.15	0.06
	106	0.71	-0.06	0.29	-0.40	0.05	-0.15	0.02	0.06	0.41	0.21
	0	0.47	0.00	0.00	0.76	0.00	0.26	0.36	0.00	0.00	0.00

References

1. Kusters RM, Singleton J, Keen DA, McGreevy R, Hayes W, *Physica B*: 1989, **155**:362.
2. von Helmholt R, Wecker J, Holzapfel B, Schultz L, Samwer K: *Phys Rev Lett* 1993, **71**:2331.
3. Jin S, Tiefel TH, McCormack M, Fastnacht RA, Ramesh R, Chen LH: *Science* 1994, **64**:413.
4. Tokura Y, Urushibara A, Moritomo Y, Arima T, Asamitsu A, Kido G, Furukawa N: *Science* 1994, **63**:3931.
5. Munoz A, Casais MT, Alonso JA, Martinez-Lope MJ, Martinez JL, Fernandez-Diaz MT: *Inorg Chem* 2001, **40**:1020.
6. Munoz A, Alonso JA, Casais MT, Martinez-Lope MJ, Martinez JL, Fernandez-Diaz MT: *J Phys: Condensed Matter* 2002, **14**:3285.
7. Kimura T, Goto T, Shintani H, Ishizaka K, Arima T, Tokura Y: *Nature London* 2003, **426**:55.
8. Kimura T, Ishihara S, Shintani H, Arima T, Takahashi KT, Ishizaka K, Tokura Y: *Phys Rev B* 2003, **68**:060403(R).
9. Goto T, Kimura T, Lawes G, Ramirez AP, Tokura Y: *Phys Rev Lett* 2004, **92**:257201.
10. Dabrowski B, Kolesnik S, Baszczuk A, Chmaissem O, Maxwell T, Mais J: *J Solid State Chem* 2005, **178**:629.
11. Martin Carron L, de Andres A: *J Alloys and Compounds* 2001, **323**:417.
12. Martin Carron L, de Andres A, Martinez-Lope MJ, Casais MT, Alonso JA: *J Alloys and Compounds* 2001, **323**:494.
13. Martin Carron L, de Andres A, Martinez-Lope MJ, Casais MT, Alonso JA: *Phys Rev B* 2002, **66**:174303.
14. Wang Wei-Ran, Xu Da Peng, Su Wen Hui: *Chin Phys Lett* 2005, **22**:705.
15. Iliev MN, Abrashev MV, Laverdiere J, Jandl S, Gospodinov MM, Wang YQ, Sun YY: *Phys Rev B* 2006, **73**:064302.
16. Gupta HC, Sharma V, Tripathi U, Rani N: *J Phys Chem Solids* 2005, **66**:1314.
17. Alonso JA, Martinez-Lope MJ, Casais MT, Fernandez-Diaz MT: *Inorg Chem* 2000, **39**:917.
18. Dabrowski B, Kolesnik S, Baszczuk A, Chmaissem O, Maxwell T, Mais J: *J Solid State Chem* 2005, **178**:629.

19. Gupta HC, Singh MK, Tiwari LM: *J Phys Chem Solids* 2003, **64**:531.
20. Rani N, Gohel VB, Gupta HC, Singh MK, Tiwari LM: *J Phys Chem Solids* 2001, **62**:1003.
21. Brown S, Gupta HC, Alonso JA, Martinez-Lope MJ: *Phys Rev B* 2004, **69**:054434.
22. Mills AJ, Littlewood PB, Shraiman BI: *Phys Rev Lett* 1995, **74**:5144.